MINING IN THE FINAL FRONTIER

Benjamin Salak¹

This paper proposes a space mining mission to a near-Earth asteroid (NEA). Included is a review of different technologies and techniques used for target selection, trajectory design, payload design, and economic feasibility. The result is a single craft designed to mine Stype near-Earth asteroid 2016 RD34. The total mission cost in terms of delta-V is 5.93 km/s. This trajectory is an optimum 2 burn outbound trajectory that relies on precise Earth/target asteroid alignment for launch. The return trajectory is modeled as a simple Hohmann transfer. The payload is designed to mine minerals using lasers with a large collection basket that can encompass small NEAs orbiting near Earth. The payload is projected to weigh 9000 kg. The total mission payload with full fuel at launch is estimated to be 45390 kg. The mission would return 12470 kg of valuable minerals. The realistic value of the cargo, based on asteroid composition, is \$7 million. Opportunities for future work are also described, leveraging payload mass reduction and improved target selection to generate profitability.

INTRODUCTION

The space mining industry is present in much of modern science fiction, from *The Expanse*, to *Dune*, and to *Star Wars* and *Star Trek*. Although space mining at the scale seen in these works of fiction is still elusive, modern science has brought space mining closer to reality. This paper aims to develop a space mining mission concept, leveraging existing technologies, and to analyze its economic viability. The analysis is broken into discrete steps: destination selection, trajectory development, payload design, and economic analysis. Each mission design step includes a literature review of current scientific and engineering understandings and a detailed analysis of the specific selection for this mission. The benefits and drawbacks of different techniques for each task to develop the mission are discussed.

¹ Graduate Student, Aerospace and Engineering Mechanics, The University of Alabama, Tuscaloosa, Alabama, 35487.

MINING TARGET SELECTION

Selecting the target for mining is the first challenge. There are three main categories to examine: lunar, near-Earth asteroids (NEAs), and main belt asteroids (MBAs).

Lunar mining is the category of mining focused on extracting resources from the Moon. There are two primary methods, surface and underground mining [1]. Surface mining focuses on collecting the firm regolith, which is the material under the loose lunar dust. Underground mining focuses on the extraction of lunar rock. The main targeted minerals are KREEPs [2]. KREEP minerals refer to potassium, rare earth elements (REEs), and phosphorous. REE elements include neodymium and dysprosium. All these minerals are critical for renewable energy technology [2].

The benefits of lunar mining are plentiful. Currently, REEs on Earth are primarily controlled by a single country. The Moon is also significantly closer than both NEAs and MBAs. The Moon's material composition is also primarily KREEPs compared to other material groups like platinum group metals (PGMs). Compared to NEAs and MBAs, the lunar surface composition is well known, which makes mining operations and returns more certain. The minable mineral content of NEAs and MBAs is not nearly as well understood [2]. Over the course of the Apollo missions, over 382 kg of regolith samples were returned that were critical to developing an understanding of planetary geology [3]. However, physical scientific data regarding asteroids are far more limited. Japan's Hayabusa2 returned a 0.2 g sample from asteroid Ryugu, and NASA's OSIRIS-Rex returned a 120 g sample from asteroid Bennu [4].

There are significant drawbacks to lunar mining as well, principally, the cultural significance the Moon holds for numerous peoples and its uniqueness compared to MBAs and NEAs [1]. Additionally, the legality of lunar mining is not yet well adjudicated.

The Moon's greatest concentrations of critical minerals are neodymium (180 ppm) and dysprosium (65 ppm) [2]. Their concentrations on Earth are 41.5 ppm and 5.2 ppm, respectively [2].

It is important to note the distinction between NEAs and MBAs. NEAs are small bodies that approach within 1.3 AU of the Sun [5]. MBAs are small bodies located in the asteroid belt, between Mars (1.52 AU) and Jupiter (5.2 AU). The asteroids are classified as different types

primarily based on light spectral analysis [6]. The main classes are C, S, and M types [7]. When the spectral analysis does not yield a clear result, where components of C, S, and M types are detected, the asteroid is classified as an X type [6].

C types are chondrite asteroids that are primarily composed of silicate rocks [7]. These are the most common asteroids with relatively high contents of metal resource targets [2]. The primary target resources are selenium, tellurium, and platinum with concentrations of 27 ppm, 3 ppm, and 1.4 ppm, respectively [2]. The concentrations of these metals on Earth are 0.05 ppm, 0.001 ppm, and 0.005 ppm, respectively [2].

S types are stony asteroids that are primarily composed of silicate and iron [7]. These asteroids contain more free metal than C types, 20% vs 10%, and are the second most common type of asteroid [2].

M types are metallic types that are primarily composed of iron and other metals [7]. These asteroids are the most resource rich and the least common. Although they have the most abundant rare resources [2], no currently classified M-type asteroids were accessible within the constraints of a study that analyzed travel time, delta-v requirements, and overall mission time [5]. The primary target resources are gallium, selenium, and platinum, with concentrations of 89 ppm, 100 ppm, and 51 ppm, respectively [1]. The concentrations of these metals on Earth are 19 ppm, 0.05 ppm, and 0.005 ppm, respectively [1]. These concentrations can also be compared to the C-type concentrations above.

NEAs are attractive as mining sites because, while their PGM content is less than that of M-type asteroids, which are primarily located in the asteroid belt [8], the concentrations are still larger than those found on Earth [2]. The delta-v cost for some NEAs is also less than that of landing on the Moon. Some NEAs can be reached from low-Earth orbit (LEO) from as low as 4 km/s [5] of delta-v, while the average is around 5.5 km/s [9]. The delta-v cost from LEO to the Moon is around 6.3 km/s [9].

The main drawback of NEA mining is the trip times, which can be substantially longer than those of lunar expeditions that optimally take only a few days. A comprehensive analysis of NEA mining feasibility pointed to trip times of up to 6 years based on asteroid and Earth positions [5].

The main benefits of mining MBAs is their larger size. Vesta, the largest asteroid in the main belt, is over 530 km in diameter [10]. The asteroid with the minimum delta-v requirement from the study of NEA objects, 2016 RD34 [5], has a best-estimate diameter of 6 m [11].

The drawback of MBA mining is the trip delta-v cost. The delta-v requirements for lunar and NEA missions are noted above, and a trip to the center of concentration of MBAs would expend 7.5 km/s to 8.5 km/s of delta-v [12].

Selecting the target for this space mining mission requires some initial reductions to the potential target list. The first reduction is to limit the targets to NEAs. Lunar mining and MBA mining are eliminated due to cultural sensitivities and delta-v requirements, respectively. Secondly, no NEA targets can be Earth crossers, which are asteroids whose orbital paths cross Earth's. These restrictions simplify the trajectory analysis. The NEAs must be S types due to their proximity to Earth and existing asteroid data. Lastly, the asteroids are selected from the list of S-type asteroids with desirable mass ratios calculated in the study, "Target Evaluation for Near-Earth Asteroid Long-Term Mining Missions" [5]. This ratio is defined as the ratio between the retrievable mass and propellant mass. The larger this ratio, the greater the quantity of desired minerals that can be extracted per quantity of propellant. The ratio defined in the study above [5] is critical for sorting all NEAs into potential candidates for mining missions. The list of potential targets is further reduced by selecting NEAs that illustrate different trajectory options. These options are the most desirable NEA, a NEA for which significant assumptions can be made based on near ideal orbital parameters for Hohmann transfer analysis, and an inclined NEA. These NEAs are listed in the following table (Table 1) with their orbital parameters, maximum material to propellant ratio [5] and comments about the characteristics that led to selection.

Table 1. NEA Orbital Elements.

					Longitude of	Argument		
	MAX Material/				Ascending	of	Mean	
Asteroid	Propellant Ratio	Eccentricity	Semi-Major	Inclination	Node	Perihelion	Anomaly [deg]	
Designation	(Rmp) [] [5]	[] [13]	Axis [au] [13]	[deg] [13]	[deg] [13]	[deg] [13]	[13]	Comments
2016	3.874	0.03465	1.046	1.957	349.6	11.033	17.69	Minimum Rmp
RD34								
2014 UV210	1.386	0.1313	1.550	0.5985	92.15	351.5	123.4	Small inclination
2000 AE205	1.171	0.1376	1.165	4.459	271.6	150.33	91.86	Large inclination

TRAJECTORY DESIGN

With the targets defined, the next stage of design, the trajectory design, can be analyzed. There are numerous trajectory options, differentiated primarily by mission concept of operations (CONOPS).

One of the largest space mining operations proposed to date is the University of Washington's space mining architecture. This architecture requires multiple space-based assets to be in place for mining. A figure with the CONOPS is shown below.

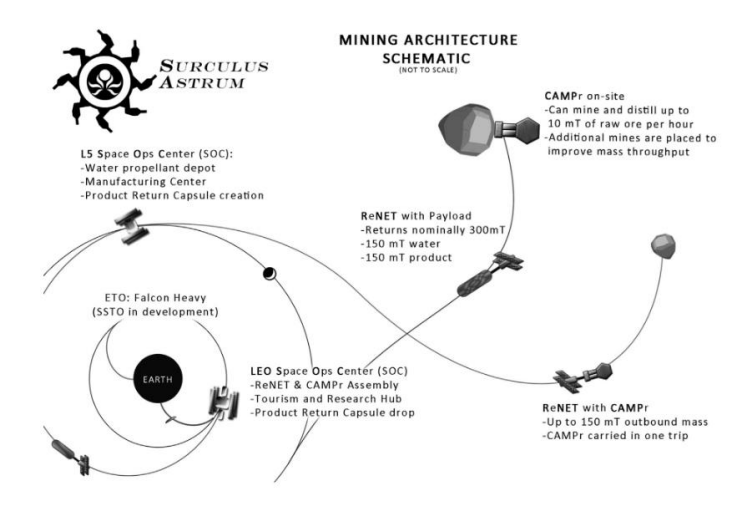


Figure 1. Surculus Astrum Mining Architecture Schematic [14].

This architecture relies on operation centers in LEO and at the L5 Lagrange point. Lagrange points are locations in space where objects remain primarily stationary. This characteristic offers strategic value to satellites and stations by reducing fuel costs [15]. The LEO Space Operations Center (SOC) is used for staging mining vehicles, mineral returns, tourism, and research [14]. The proposed L5 SOC is used for storage and transfer of minerals for return to Earth and processing the observations from prospector missions [14]. The mining is accomplished using a proposed mining payload called CAMPr. The CAMPr is transported to the target asteroid by a nuclear tug called ReNET [14]. The ReNET returns from the target asteroid with a payload of minerals that are processed at the SOCs and returned to Earth. Of the proposed trajectories analyzed, this is the most ambitious, relying on multiple initial orbiting SOCs, a cargo tug in an Earth-asteroid transfer orbit, and numerous mining payloads conducting operations on the asteroid surface.

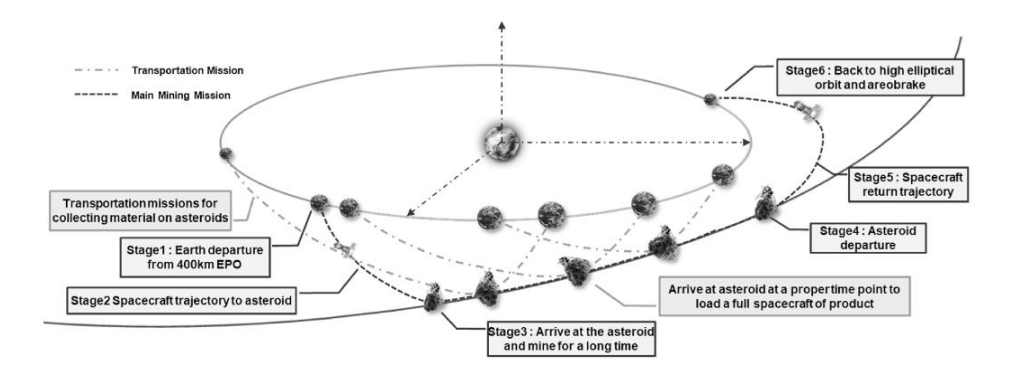


Figure 2. Notional NEA Mining Architecture Schematic [5].

A significantly reduced mission CONOPS is shown above (Figure 2). This proposed mining operation relies on a single space mining payload that is emptied multiple times with transportation missions to return the ore [5]. The transportation options discussed in the University of New South Wales proposed trajectory vary depending on whether in situ resource utilization (ISRU), like refining, takes place or not [5]. Multiple transport missions are required since it is challenging to transport all the mining equipment and have excess propellant to deliver all the mined material back to Earth (especially if the mission time resulting from orbital parameters is exceedingly long) [5]. Aerobraking is also proposed in this study as a way to reduce the delta-v required to safely enter an Earth orbit [5].

Another method to reduce the delta-v required for an asteroid mission trajectory is with gravity assists. An example of a trajectory to an asteroid that relied on a gravity assist is the OSIRIS-REx mission, whose trajectory is shown below [16].

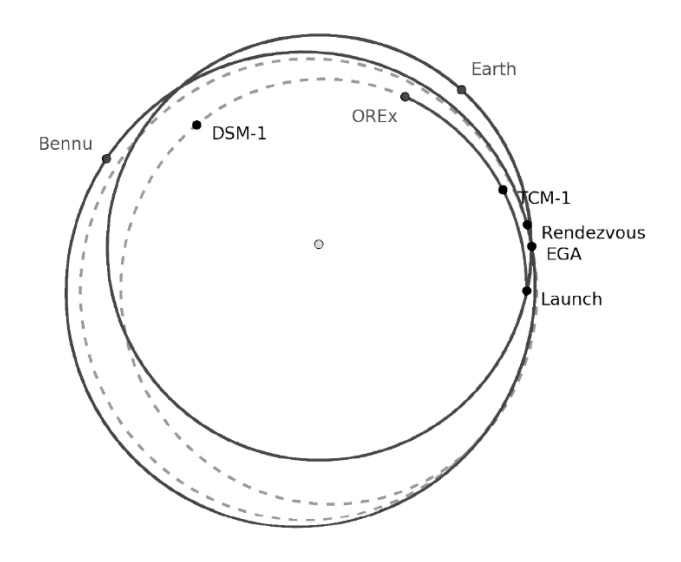


Figure 3. NASA OSIRIS-REx Orbital Trajectory [16].

While en route to asteroid Bennu to capture and return an asteroid sample, the OSIRIS-REx spacecraft used Earth's gravitational force to redirect its trajectory to shift its orbital plane to the orbital plane of the target asteroid (Figure 3).

The least complex trajectory proposed for space mining is the mining CONOPS from AstroForge (Figure 4). Its trajectory is direct to NEAs without any gravity assists or aerobraking. Unlike other CONOPS that require trajectory design for transport tugs or transport missions to the asteroid, AstroForge relies on ISRU [18].



Figure 4. AstroForge Orbital Trajectory [18]

The benefit of this concept is the simplicity of the trajectory. To achieve profitability and large-scale asteroid mining operations, AstroForge will have many of these autonomous, self-sufficient mining operations underway simultaneously [18].

For the space mining mission under development, the simple trajectory used by AstroForge was selected. The complexity of the other proposed space mining mission trajectories and the required support structures and systems to enable space mining make a space mining mission from one Earth-based rocket launch impossible.

The trajectories to each asteroid using this space mining CONOPS must be computed. The computations are essential as the delta-v required to reach the asteroid will determine how much propellant is required. The less propellant required, the more mass can be allocated to storing the valuable minerals collected from the asteroid. To estimate the delta-v required to arrive at the asteroid, a 2-burn maneuver is employed. This 2-burn maneuver was developed for MBAs, but the equations can also be used to estimate delta-v requirements for non-Earth crossing NEAs [12].

The assumptions for this model are that the burns were performed at high thrust and the orbital changes happen instantaneously. The 2-burn method shown below is a derivation from patched conics to model with fidelity the effects of different gravitational bodies on the spacecraft.

The equation for Burn 1 is a combination of a Hohmann transfer and the required velocity for Earth escape. Because inclination is considered in this analysis, the Hohmann transfer does not start at periapsis but instead aligns 180 degrees from the ascending or descending node to ensure that the spacecraft arrives when the asteroid is in plane. Equation 1 is shown below [12]:

$$\Delta v_1 = \left(\left(\frac{2 \cdot \mu_{Sun}}{a_{Earth}} - \frac{2 \cdot \mu_{Sun}}{r_{node} + a_{Earth}} \right)^{\frac{1}{2}} - v_{Earth} \right)^2 + v_{esc}^2 \right)^{\frac{1}{2}} - v_{park} \tag{1}$$

In the above equation:

 μ_{Sun} is the standard gravitational parameter for the sun.

 a_{Earth} is the semi major axis of the Earth's orbit.

 r_{node} is the orbital radius at either the ascending or descending node. The node is selected based on which is farthest from the Sun to maximize the Oberth effect and to conduct orbit-raising maneuvers when the spacecraft velocity is highest.

 v_{Earth} is the velocity of the Earth (at time of Burn 1).

 v_{esc} is the escape velocity from Earth starting from the parking orbit.

 v_{park} is the velocity of the satellite in the parking orbit.

To calculate the velocity of Earth, the following equation (Equation 2) can be used [19]:

$$\frac{v^2}{2} - \frac{\mu_{Sun}}{r} = \frac{-\mu_{Sun}}{2 \cdot a} \tag{2}$$

This can be solved for velocity on the left-hand side, as shown below (Equation 3):

$$v = \sqrt{\frac{2 \cdot \mu_{Sun}}{r} - \frac{\mu_{Sun}}{a}} \tag{3}$$

The radius of the Earth's orbit is dependent on the pre-burn positions of the Earth and the target asteroid. The radius of the orbit can be found with the following equation (Equation 4):

$$r = a \cdot \frac{1 - e^2}{1 + e \cdot \cos(\theta)} \tag{4}$$

For these orbital maneuvers to be effective, the Earth must be positioned along either the ascending or descending node, whichever is closer to the Sun, to maximize the Oberth effect. Node selection is dependent on the target asteroid's orbit. To effectively relate the orbits of Earth and the target asteroid, the true anomaly, right ascension of the ascending node, and the argument of perigee are required. The Small Body Database Lookup from NASA's JPL was the source for the orbital parameters of the target asteroids. The database includes the longitude of the ascending node, argument of perihelion, and the mean anomaly. The longitude of the ascending node and the argument of perihelion are identical to the right ascension of the ascending node (RAAN) and the argument of perigee.

The desired true anomaly can be determined from the geometry of the RAAN and the argument of perigee. Now the radius of the Earth's orbit at a given time can be computed and then the Earth's velocity can be calculated.

To calculate v_{esc} for the spacecraft from the parking orbit, the following equation (Equation 5) can be used [19]:

$$v_{esc} = \sqrt{\frac{2 \cdot \mu_{Earth}}{r_{park}}} \tag{5}$$

To calculate v_{park} , which is the velocity of the spacecraft in its circular (assumed) parking orbit, the following equation (Equation 6) can be used [19]:

$$v_{park} = \sqrt{\frac{\mu_{Earth}}{r_{park}}} \tag{6}$$

 r_{node} is the orbital radius when the true anomaly of the asteroid is at the RAAN. Based on the definitions of RAAN, argument of perigee, and true anomaly, this alignment occurs when true anomaly (θ) is equal to 360 – argument of perigee (ω). The same equation used to find Earth's orbital radius, Equation 4, can be used to find this value (with the asteroid orbital parameters used in lieu of Earth's).

For clarity, an NEA potential mining target from the target selection, 2000 AE205, is shown below as an example [13]. The figure (Figure 5) has been annotated to show the relevant orbital information required to calculate Burn 1.

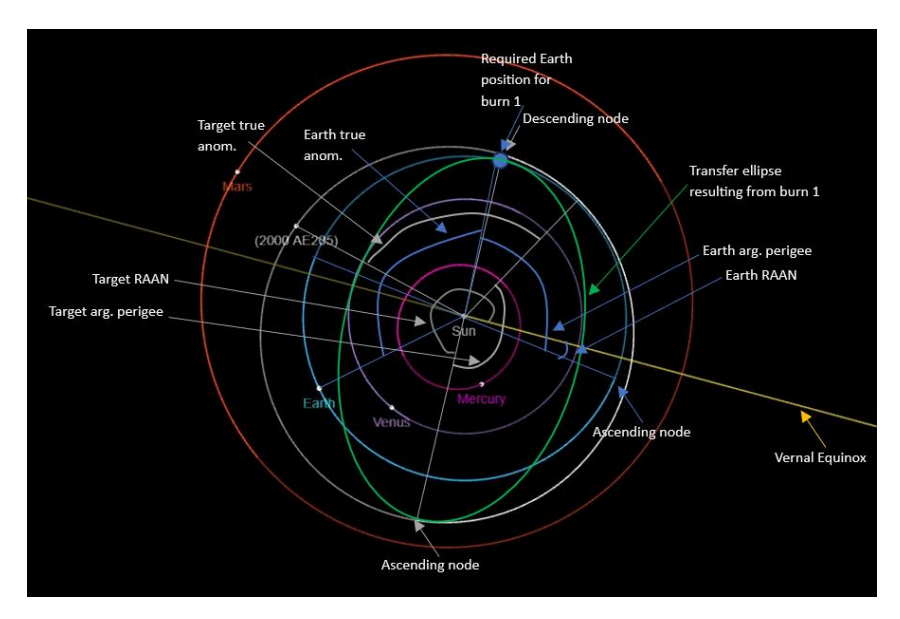


Figure 5. 2000 AE205 Outbound Trajectory.

To find Earth's velocity and position at the time of Burn 1 at the descending node, 180 degrees can be subtracted from the RAAN of the asteroid to find the descending node's angle from the vernal equinox. The Earth's angular distance from the vernal equinox must be equal to the result of the subtraction. The angular distance from the vernal equinox is the sum of the RAAN, the argument of perigee, and the true anomaly. The result in this case is approximately 0 degrees (-0.0865), so the burn effectively takes place at Earth perigee.

The radius of Earth's orbit can be computed with Equation 4. This yields $147 \cdot 10^6$ km. The velocity of Earth at this point in the orbit can be computed by using Equation 3. The result is a velocity of 30.28 km/s. By using Equation 5, the escape velocity of the mining craft in a 300 km altitude parking orbit is determined to be 10.92 km/s. By using Equation 6, the velocity of the craft in the parking orbit is determined to be 7.72 km/s.

The delta-v required for Burn 1 can now be computed with Equation 1, which results in a burn of 3.2856 km/s.

Next, the equation for Burn 2 can be analyzed and the result computed. Below is the equation (Equation 7) for this burn [12]:

$$\Delta v_2 = \sqrt{v_{craft} + v_{asteroid} - 2 \cdot v_{craft} \cdot v_{asteroid} \cdot \cos(\psi)}$$
 (7)

Where:

 v_{craft} is the velocity of the spacecraft at the apogee of the transfer ellipse.

 $v_{asteroid}$ is the velocity of the asteroid at the ascending node, which coincides with the apogee of the transfer ellipse.

 ψ is the difference in inclination between the respective orbits (transfer ellipse and asteroid orbit).

The figure below (Figure 6) illustrates the conditions before Burn 2.

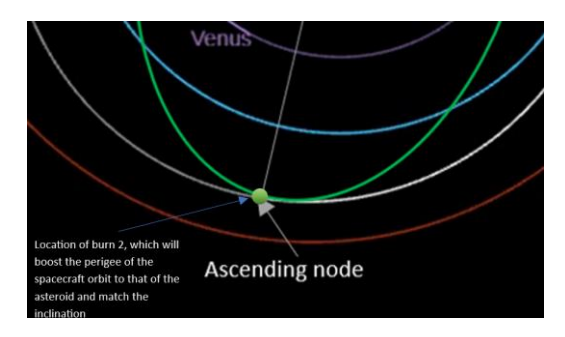


Figure 6. Annotated NEA Burn 2 Orbital Alignment.

 v_{craft} is at apogee, where true anomaly is equal to 180 degrees, and the orbital radius is equal to that of r_{node} and can be computed with Equation 4, with transfer ellipse parameters used instead of Earth's.

 $v_{asteroid}$ can be computed with Equation 3, with parameters adjusted to reflect the asteroid instead of Earth, and the true anomaly used to compute r_{node} . For the example NEA, the v_{craft} is 24.27 km/s, $v_{asteroid}$ is 24.6056 km/s, and ψ is the inclination difference of 4.4589 degrees. This process can be repeated to gain an understanding of the remaining candidate target velocity requirements. The transfer orbit for Burn 1 is shown for each below (Figure 7 and Figure 8), and the Burn 1 and Burn 2 results are tabulated (Table 2).

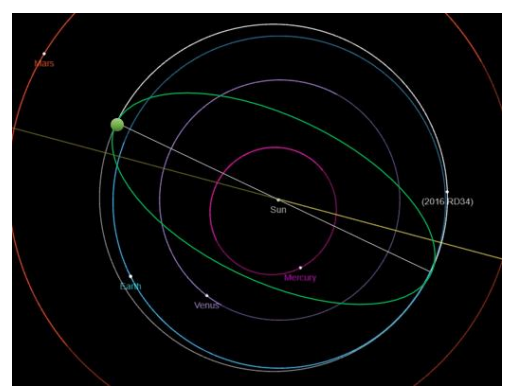


Figure 7. 2016 RD34 Outbound Trajectory.



Figure 8. 2014 UV210 Outbound Trajectory.

Table 2. NEA Outbound Delta-V Computations.

NEA []	Departure node [ascending or descending]	$\Delta v_1 + \Delta v_2 \text{ [km/s]}$
2016 RD34	Descending	4.3858
2014 UV210	Ascending	5.2707
2000 AE205	Descending	5.2154

As referenced in the assumptions with the equations, these are ideal two-burn trajectories designed to minimize the delta-v cost. It is important to understand how often these transfer windows will occur, as this dictates the mission duration and wait time using this burn approach. The transfer window can be computed using the synodic period, which represents how long it will take for a given configuration of the asteroid, relative to Earth, to reoccur. The desired position of the asteroid is such that when the spacecraft is launched on its transfer ellipse, it arrives at the descending or ascending node of the asteroid's orbit at the same time as the asteroid. This period can be calculated with the following equation (Equation 8) [19]:

$$T_{synodic} = \frac{T_{Earth} \cdot T_{Asteroid}}{|T_{Earth} - T_{Asteroid}|} \tag{8}$$

The periods for each NEA are referenced in the table below. The times for each launch scenario relative to the position of the target asteroid are shown in the table below (Table 3).

NEA []	Orbital Period [days]	Synodic Period [years]
2016 RD34	390	15.75
2014 UV210	453	5.16
2000 AE205	459	4.90

Table 3. NEA Orbital and Synodic Periods.

Before selecting a target asteroid, the mass of each target asteroid must be quantified. Since data are limited to emission spectra and observations, the "best guess diameter" is used to estimate the potential amount of material for mineral extraction. The larger the diameter, the greater the quantity of extractable minerals. Shown in the table below (Table 4) are the estimated diameters of each target NEA.

Table 4. NEA "Best Guess" Diameters.

NEA []	Diameter ("best guess estimate") [m]
2016 RD34	6 [11]
2014 UV210	7-32 [20]
2000 AE205	66-149 [21]

Due to delta-v constraints, 2016 RD34 is selected as the target for the mission. It offers enough mass for extraction, without needing numerous resupply or transport missions. It also requires the least delta-v. These factors mean more minerals can be extracted for the return journey. The major drawback is that the synodic period is significantly longer than those of the other target candidates as a result of the similarity of its orbit to Earth's. Since the CONOPS are not for multiple missions and only a single all-in-one mining craft is used, this drawback is mitigated as much as possible.

With the target selected, a return burn can be estimated. Since the diameter of the asteroid is so small, the only delta-v considered will be the adjustment to the orbit to reduce the perigee to that of Earth's. Since it is a nonstop return trip, the direct reduction to Earth's perigee will ensure that aerobraking will deorbit the spacecraft with its payload to Earth. A simple Hohmann transfer can be assumed with a burn at the ascending node of the NEA to the radius of Earth's orbit at the descending node of the asteroid. The speed of the asteroid at the descending node and that of Earth at the common apse line of the asteroid's descending node can be found using the orbital radius Equation 4 and orbital velocity Equation 3. The resulting delta-v required is 1.54 km/s. This means that the two burns to transit to the NEA are approximately 74% of the total propellant needed when compared with the return burn delta-v.

PAYLOAD DESIGN

To effectively design a payload for space mining, the mining method must be established. There are several possible methods for mining minerals from an asteroid. The principal mining techniques include strip mining, tunnel mining, biomining, optical mining, and robotic mechanical extraction. There are multiple devices that can remove regolith, or surface material, from the target. These devices include a slusher, a bladed roller, a conveyer belt collection system (for especially loose regolith), a conveyer belt collection system augmented with an inclined plane, a scarifier and inclined plane, and a buck wheel collection system [1]. These design concepts are based on Earth strip-mining machines and require frequent maintenance and lots of material to process but excel in rapidly excavating and uncovering mineral-rich regolith.

Tunnel mining is similarly rooted in Earth-based mining techniques involving three steps: drilling, blasting, and ore removal [1]. An example of a tunnel-mining device is a caterpillar-crawler electric-powered vehicle [1]. For the blasting, there are substantial risks to using

explosives in a confined underground mine [1], especially when the mining mission will be controlled remotely, with no humans supervising the operation. A benefit of the underground mining is the potential to convert it to a human-habitable base, as the tunnels would provide shelter from cosmic rays. However, these machines have a lot of moving parts [1] and have never been used in zero gravity. The fewer moving parts, the less maintenance required.

Biomining refers to the use of microorganisms to extract desired minerals from a medium [22]. Biomining has been used on Earth to extract copper, zinc, cobalt, and other materials [22]. The benefits of biomining are its ability to extract minerals from harsh environments on Earth. The limitations are that current closed bioreactors would only be able to mine iron and nickel on NEAs [22] and not PGMs (the most lucrative minerals). Secondly, the microorganisms are not adapted to the space environment [22], which leaves significant risk for the success of the mining mission.

Optical mining is the process of ablating material with focused light. This process can be conducted from above the target asteroid or while the spacecraft is secured to the asteroid.

Anchoring to an asteroid adds risk due to potential instability resulting from torques and a lack of knowledge about the landing area and overall asteroid topography [23]. The benefits of anchoring are less energy lost due to the distance from the primary laser source and the target for mining and the more complete collection of valuable spatter generated from the mining process.

Current technology has demonstrated that lasers can be used from a distance to ablate material into spatter [23]. This spatter can then be collected by the spacecraft and further processed.

AstroForge has proposed the use of laser ablation as a collection method for their standalone space mining solution, which anchors magnetically to the asteroid [18]. TransAstra has also proposed a method for excavating with laser ablation. To mitigate spatter that is not captured in collection, TransAstra has a proposal to surround the minable surface with a capture bag to ensure minimal loss [24]. This bag can work on asteroids as large as a house [24].

Robotic mechanical extraction covers several types of mechanical extracting methods, albeit on a smaller scale than that of strip mining or tunnel mining. Examples of mechanical extraction include mechanical stress, spark cratering, and drilling [1]. Mechanical stress is the process of using force to exceed the strength of the rock and break it into chunks through fracturing the material [1]. Due to the low gravity, dust and potentially valuable desired minerals are perturbed,

possibly moving out of the collection range [1]. To counter this problem, an orbiting collection bag can be placed above the fracturing area to mitigate the loss of valuable regolith [1], but this step adds complexity by introducing multiple collaborating mining systems. Spark cratering is a variant on mechanical stress that relies on electric differential to generate the fracturing force instead of blunt mechanical force [1].

For the space mining mission under development, laser ablation was chosen because of the limited moving parts and the ability to use nuclear or electric solar power freely in space to power a high power, 300 W + [23] laser for mining applications. While TransAstra's mining focuses on water mining for propellant generation, the 6 m diameter NEA is an optimum candidate for a fusion between AstroForge's ISRU refining and TransAstra's capture bag technology. This tech fusion is the primary system for mining and capturing the valuable minerals. Shown below on the left (Figure 9) is TransAstra's capture bag technology. Shown on the right (Figure 10) is an image of AstroForge's prototype ablation and ISRU unit currently undergoing testing in orbit [18].



Figure 9. TransAstra HoneyBee [24].



Figure 10. AstroForge ISRU & Ablation [18].

Due to the single spacecraft trajectory design and CONOPS, ISRU is used to ensure only the valuable PGMs and REEs are returned to Earth, and no delta-v is wasted hauling waste regolith back to Earth.

To finalize the overall payload architecture, a mass budget must be generated. This budget is based on current launch vehicle performance, delta-v required for the mission, mining equipment weight, and the quantity of returned minerals. An estimate is needed for the mass of the target asteroid, given its diameter. The density of the target NEA, which is S type, is approximately 2.71 g/cm³ which can be rewritten as 2710 kg/m³ [25]. The shape of the target asteroid can be

assumed to be spherical, and the equation for the volume of the sphere (Equation 9), below, can be used to estimate the volume.

$$v_{sphere} = \frac{4}{3} \cdot \pi \cdot \left(\frac{d_{asteroid}}{2}\right)^3 \tag{9}$$

The resulting volume of target asteroid 2016 RD34 is 113 m³. With the above estimated density, the total mass of the asteroid is estimated to be 306493 kg. NASA estimates that a 650000 kg S-type asteroid contains 50 kg of platinum, which in the case of the target asteroid reduces to 23.5 kg of platinum [26]. The remaining metals that can be extracted from the S type are iron (6% to 19% of mass), nickel (1% to 2%), and cobalt (0.1%). Volatiles such as carbon (3%) and sulfur (2%) and numerous mineral oxides can also be collected. The collectable mass from the target asteroid for metals, volatiles, and oxides are tabulated below (Table 5).

Table 5. NEA 2016 RD34 Material Composition.

		Type	Percent of mass	
Linear formula [29]	Name [29]	[29]	[%][29]	Mass [kg]
Fe	Iron	metal	18.02	55230.0386
Ni	Nickel	metal	2	6129.86
Co	Cobalt	metal	0.1	306.493
C	Carbon	volatile	3	9194.79
S	Sulfur	volatile	1.5	4597.395
FeO	Wustite	oxide	10	30649.3
SiO2	Silicon dioxide	oxide	38	116467.34
MgO	Magnesium oxide	oxide	24	73558.32
Al2O3	Aluminum oxide	oxide	2.1	6436.353
Na2O	Sodium oxide	oxide	0.9	2758.437
K2O	Potassium dioxide	oxide	0.1	306.493
P2O5	Phosphorous pentoxide	oxide	0.28	858.1804
PGM	Platinum Group Metal	metals	DERIVED	23.5 [26]
TOTAL				
EXTRACTABLE				
MASS [kg]			100	306516.5

There is clearly more mass available for extraction than what a payload could return to Earth. Economically, only the most valuable oxides and PGMs will be collected during mining operations. To put a limit on the amount collected, the total payload mass must be determined. This is limited by the overall mass able to be inserted into orbit from a launch vehicle. Since the

intention is to return the minerals to Earth, the entire cargo must fit in the spacecraft so a heat shield can protect it on re-entry. The payloads that each of the main launch vehicles can lift into orbit (notional LEO orbit) and the volume of the payload space are tabulated below (Table 6).

Table 6. Launch Vehicle Specifications.

Launch vehicle	Payload fairing diameter	Volume [m ³]	Payload to LEO
	(PLF) [m]		[metric tons]
Falcon 9	4.6 m [5]	142 [5]	22.8 [31]
Falcon Heavy	5.2 m [32]	145 [32]	63.8 [32]
Delta IV	5 m [5]	233 [5]	28.3 [33]
Vulcan	5.4 m [5]	216 [5]	27.2 [30]
Arianne 64	6 m [5]	240 [5]	21 [34]
New Glenn	7 m [5]	458 [5]	45 [37]
SLS Block 1	5 m [36]	229 [36]	95 [35]
SLS Block 2 (excluded from average)	10 m [36]	1320 [36]	130 [35]
Average (approximate)	5.6	250	46

To scope the analysis, a notional payload mass is assumed. The mass of the TransAstra HoneyBee collection system and support structure is 5000 kg [38]. To store the cargo and represent the control section, the Cygnus probe mass is used as an estimate. The resupply probe weight is approximately 1600 kg [39]. A heat shield, which weighs approximately 1400 kg [40], is included. An extra 1000 kg is added to account for increased structural integrity and a larger engine. This brings the payload dry mass to 9000 kg. For reference, The Hubble Space Telescope weighs 10000 kg.

The return delta-v must be optimized to ensure maximum ore return. For propulsion, a notional ISP of 470 is assumed [41]. The rocket equation can be used to determine the optimum mass of cargo and propellant. The equation is shown below (Equation 10) as written for the return burn trajectory.

$$\Delta v_{return} = I_{sp} \cdot g_0 \cdot \ln \left(\frac{m_{payload} + m_{returnFuel} + m_{cargo}}{m_{payload} + m_{cargo}} \right)$$
 (10)

Since there are two unknowns, this equation can be solved iteratively. To bound the problem, a total maximum mass of 46000 kg is assumed (average max payload mass of analyzed launch vehicles). This is the average maximum weight that can be put into orbit so the fuel load cannot exceed this value and is less than the re-entry weight of the space shuttle, so the technology exists to ensure the large mass of valuable mineral cargo can safely reenter the atmosphere.

The result for the return trajectory is below (Figure 11). This result is also bounded by the outbound trajectory since the fuel reserves required for the return trip must be accounted for during the outbound mission phase.

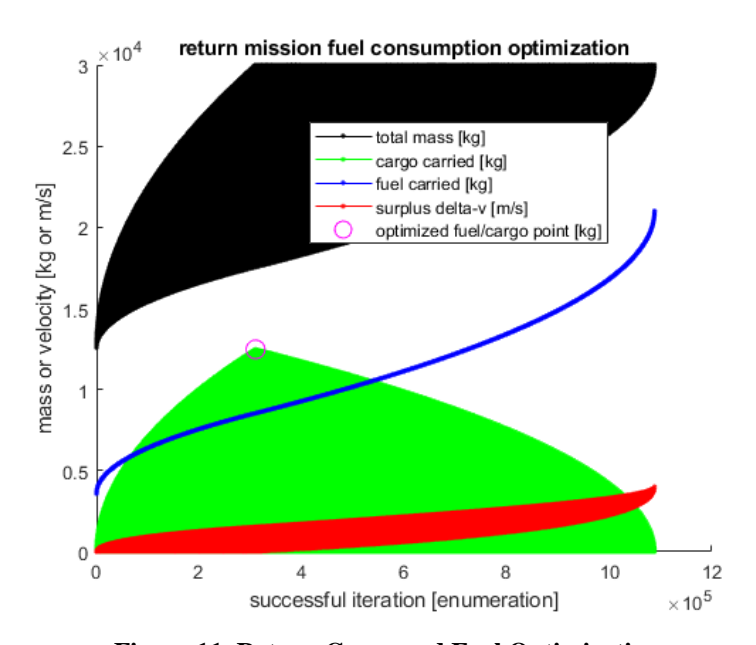


Figure 11. Return Cargo and Fuel Optimization.

The result is a fuel load of 8530 kg to transport 12470 kg of minerals (and the payload structure) back to Earth. There is a slight delta-v surplus in this budget of 0.692 m/s of delta-v. For the outbound journey the following equation can be used:

$$\Delta v_{outbound} = I_{sp} \cdot g_0 \cdot \ln \left(\frac{m_{payload} + m_{returnFuel} + m_{outoundFuel}}{m_{payload} + m_{returnFuel}} \right)$$
(11)

At this point, the dependency on the return mass requirements arises. This solution can also be optimized as shown in the plot (Figure 12).

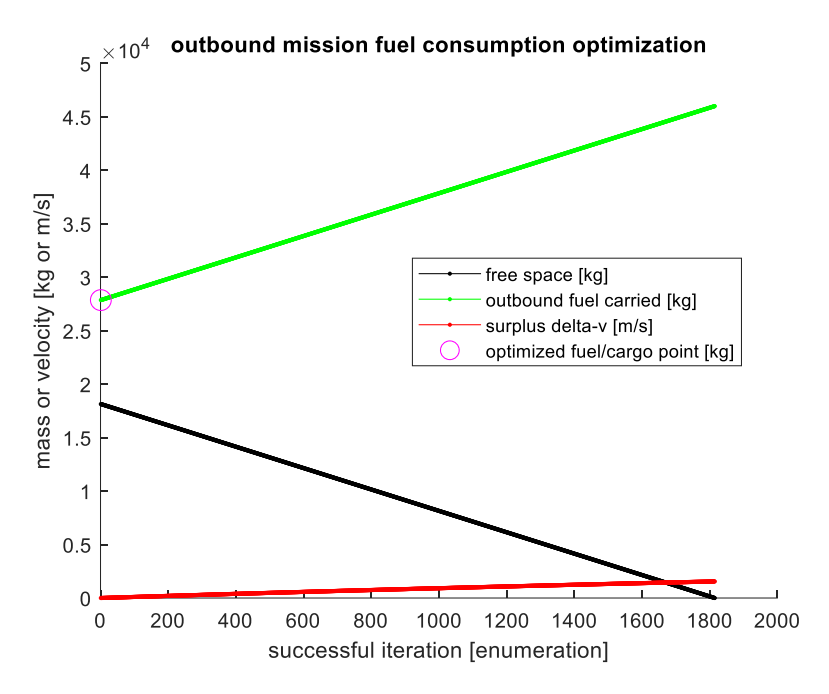


Figure 12. Outbound Launch Mass and Fuel Optimization.

The result is a launch payload mass of 45390 kg and a spacecraft mass return mass of 21470 kg. Of the initial mass requirement, this mission concept uses 98% of the allocated launch mass. The mass composition is primarily from the payload mass (9000 kg), outbound fuel (27860 kg), and return fuel (8530 kg).

PROFITABILITY

With the payload mining concept, mass requirements, and fuel loads computed, the profitability of the mission can be analyzed. The previous mining material table has been supplemented with cost data for each material and how much total value is present on the target asteroid (Table 7).

Table 7. Asteroid Profitability.

			Percent					
Linear formula			of mass	Mass [kg]	Cost per unit	Unit		Value
[29]	Name [29]	Type [29]	[%][29]	[29]	[\$]	[kg]	Total value	per kg
Fe	Iron	metal	18.02	55230.0386	36.8 [28]	5	406493.084	7.36
Ni	Nickel	metal	2	6129.86	15.33 [28]	1	93970.7538	15.33
Co	Cobalt	metal	0.1	306.493	33.7 [28]	1	10328.8141	33.7
С	Carbon	volatile	3	9194.79	2.4 [47]	1	1121.76438	2.4
S	Sulfur	volatile	1.5	4597.395	0.13 [45]	1	425.718777	0.13
FeO	Wustite	oxide	10	30649.3	2 [46]	1	61298.6	6.6
SiO2	Silicon dioxide	oxide	38	116467.34	635 [27]	5	14791352.2	127

MgO	magnesium oxide	oxide	24	73558.32	138 [27]	1	10151048.2	138
A12O3	Aluminum oxide	oxide	2.1	6436.353	249 [27]	1	1602651.9	249
Na2O	sodium oxide	oxide	0.9	2758.437	388 [27]	0.25	4281094.22	1552
K2O	potassium dioxide	oxide	0.1	306.493	205 [27]	0.25	251324.26	820
P2O5	phosphorous pentoxide	oxide	0.28	858.1804	304 [27]	0.25	1043547.37	1216
PGM	Platinum Group Metal	PGM	N/A	23.5	31,217.65 [42]	1	733614.775	31217.65
TOTAL				306516.5				
EXTRACTABLE MASS [KG]			100				33428271.6	
VALUE IN								
MILLIONS OF ASTEROID [\$]							33.4282716	

This data set can be used for two cases, first, an idealized case where the target asteroid has a different set of material properties and all 12470 kg of cargo can be filled with PGMs. This idealized scenario would result in a cargo value of \$389,248,095. For this to be realistic, the asteroid would need to be 500 times bigger than it is. The more realistic estimate is that the spacecraft captures and refines a cargo load of the high-value materials (more than \$200 per kg) and discards the rest. This estimate would make the cargo worth \$7,178,617. This scenario would involve mining the entire asteroid and would leave 2000 kg of empty space in the cargo hold. A baseline scenario is that the spacecraft cannot sort and extract a representative amount of all material present on the asteroid. This baseline scenario values the cargo at approximately \$2 million.

The next step is to evaluate the cost of the mission. Instead of assigning a value to the payload, due to the limited realistic returns of \$2 million to \$7 million of cargo value, looking at launch cost will suffice. Since the launch mass is approximately 45 metric tons, the currently available launch vehicles are the Falcon Heavy and the New Glenn. The Falcon Heavy costs \$90 million to launch [43] and the New Glenn costs \$70 million to launch [44]. These launch vehicles cost more than the realistic mining cases. The unrealistic full cargo hold of PGMs remains highly profitable.

CONCLUSION

The final mission design can be summarized as follows. The mining mission is a single craft designed to mine S-type, near-Earth asteroid 2016 RD34. The total mission cost in terms of delta-v is 5.93 km/s. This trajectory is an optimum two-burn outbound trajectory that relies on

precise Earth/target asteroid alignment for launch. The payload is designed to mine with lasers surrounded by a large collection superstructure that can encompass small NEAs orbiting near Earth. The payload is projected to weight 9000 kg. The total mission payload with full fuel at launch is estimated to be 45390 kg. The mission would return 12470 kg of valuable minerals. The realistic value of the cargo is \$7 million, which is far less than the \$70 million to \$90 million required to launch such a heavy payload. If the entire cargo hold were filled with PGMs, the mission would return \$389 million in minerals. In this paper, different techniques for target selection, mission planning, and payload design were analyzed. The resulting mission plan was the result of weighing the benefits and drawbacks of different techniques and the potential for economic viability.

There are several opportunities for improvement on the payload. The payload mass estimate is 9000 kg to account for the mining equipment, control section, engines, fuel tanks, and supports for the cargo hold. If this estimate could be reduced to 6000 kg, the cargo that can be returned would be 27000 kg. This modification would increase profits dramatically on all three estimates. The optimizations for this payload mass are shown in Figures 13 and 14. Opportunity for further work is the reduction of the 900 kg notional payload to the 6000 kg mass allocation.

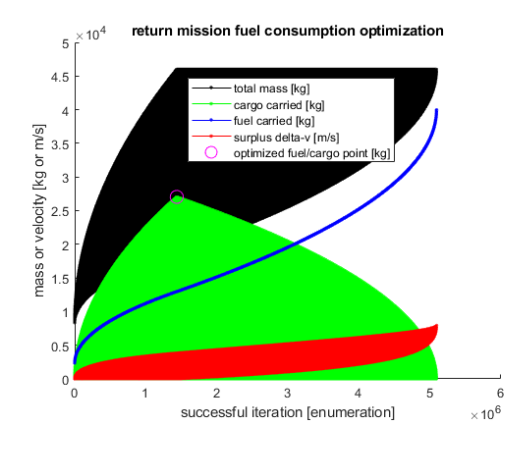


Figure 13. Return Launch Mass and Fuel Optimization.

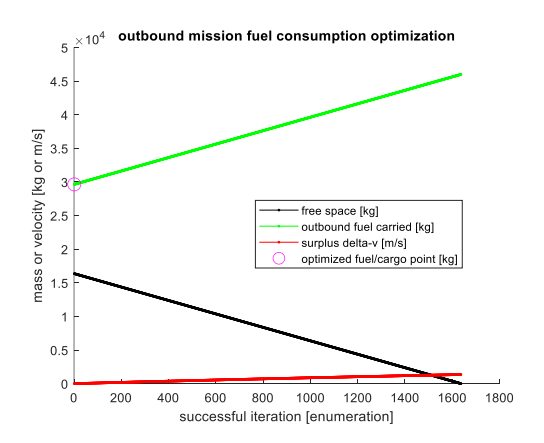


Figure 14. Inbound Launch Mass and Fuel Optimization.

For a full cargo hold, with no filtering, the estimated profit is \$3.63 million. The estimated high-value refined return would be limited to the total mass of the asteroid (since to fill up the entire cargo hold, the concentrations would have to be substantially higher or the asteroid much larger).

This return would be \$5.5 million. If the asteroid were large enough to fill up the entire cargo hold with valuable concentrations, the cargo value would be around \$36 million. Lastly, if the hold were filled with PGMs, with the understanding that the asteroid would have to be incredibly large, larger than main belt asteroids, the value would be \$842 million. This extrapolation shows that space mining is possible, and it has a chance to be profitable; however, the dry mass of the payload must be minimized, and the quality of the asteroid to mine must be exceptional. It is essential that prospector ships evaluate the detailed properties of the asteroid before a large payload is sent on a long mission to extract the valuable minerals. As technology evolves closer to the profitability of science fiction's space mining, the required mass to extract the minerals will decrease.

REFERENCES

- [1] Sivolella, D. (2019). Space Mining and Manufacturing: Off-World Resources and Revolutionary Engineering Techniques. Chichester, UK: Springer.
- [2] Dallas, J.A., Raval, S., Saydam, S. and Dempster, A.G. (2021). "Investigating Extraterrestrial Bodies as a Source of Critical Minerals for Renewable Energy Technology." *Acta Astronautica*, Vol. 186, pp. 74-86.
- [3] Jawin, E. (2019). "Apollo's Bounty: The Science of the Moon Rocks." *Scientific American*. https://www.scientificamerican.com/article/apollos-bounty-the-science-of-the-moon-rocks/
- [4] Lakdawalla, E. (2020). "Sample Return Roundup: 3 Countries and 4 Missions to Return Samples from Space." *The Planetary Report*. https://www.planetary.org/articles/sample-return-roundup-2020
- [5] Xie, R., Bennett, N.J., and Dempster, A.G. (2021). "Target Evaluation for Near Earth Asteroid Long-Term Mining Missions." *Acta Astronautica*, Vol. 181, pp. 249-270.
- [6] Fornasier, S., Clark, B.E. and Dotto, E. (2011). "Spectroscopic Survey of X-type Asteroids." *Icarus*, Vol. 214, No. 1, pp. 131-146.
- [7] NASA. (n.d.) "Asteroid Facts." https://science.nasa.gov/solar-system/asteroids/facts/
- [8] Bartlett, R.J. (2020) "Different Types of Asteroids (C, S, and M) The Definitive Guide." *Astronomy Source*. https://astronomysource.com/different-types-of-asteroids/#:~:text=M%2Dtype%20asteroids%20are%20typically,contain%20small%20amounts%20of%20stone.
- [9] Sonter, M.J. (1997). "The Technical and Economic Feasibility of Mining the Near-Earth Asteroids." *Acta Astronautica*, Vol. 41, Nos. 4-10, pp. 637-647.
- [10] NASA. (n.d.) "Asteroids." https://science.nasa.gov/solar-system/asteroids/
- [11] Zambrano-Marin, L.F., Howell, E.S., Marshall, S.E., Giorgini, J., and Venditti, F.C.F. (2024). "The Fastest Rotators: Near-Earth Asteroids Observed with the Arecibo Planetary Radar System." *Icarus*, Vol. 415.
- [12] Taylor, A., McDowell, J.C., and Elvis, M. (2018). "A Delta-V Map of the Known Main Belt Asteroids." *Acta Astronautica*, Vol. 146, pp. 73-82.
- [13] NASA Jet Propulsion Laboratory, California Institute of Technology. Small-Body Database Lookup. https://ssd.jpl.nasa.gov/tools/sbdb_lookup.html#/
- [14] Andrews, D.G., et al. (2015). "Defining a Successful Commercial Asteroid Mining Program." Acta Astronautica, Vol. 108, pp. 106-118.
- [15] NASA. (n.d.) "What is a Lagrange Point?" https://science.nasa.gov/resource/what-is-a-lagrange-point/
- [16] Green, J. (2017). "Planetary Division Status Report" [Slide presentation]. National Science Foundation. https://www.nsf.gov/attachments/189767/public/Green NASA Planetary AAAC V3-comp.pdf
- [17] O'Neill, I. (2017). "How Gravity Assists Work: Asteroid Probe's 'Interplanetary Billiards' Flyby Explained." https://www.space.com/38226-how-gravity-assists-work-osiris-rex.html
- [18] AstroForge, (2023). Written Testimony to the Committee on Natural Resources Subcommittee on Oversight and Investigations, U.S. House of Representatives, on the mineral supply chain and the new space race. https://www.congress.gov/118/meeting/house/116618/documents/HHRG-118-III5-20231212-SD003.pdf
- [19] Curtis, H. (2014). Orbital Mechanics for Engineering Students, 3rd ed. Amsterdam: Elsevier.
- [20] Space Reference. (2021) "2014 UV210: Very Small Apollo-Class Asteroid." https://www.spacereference.org/asteroid/2014-uv210
- [21] European Space Agency. "Asteroid Ranking for the M-ARGO mission." (2017). https://www.esa.int/gsp/ACT/projects/lt_to_NEA/rankings/

- [22] Gumulya, Y., Lis Zea, L., and Kaksonen, A.H. (2022). "In Situ Resource Utilisation: The Potential for Space Biomining." *Minerals Engineering*, Vol. 176.
- [23] Anthony, N., et al. (2021). "Laser Processing of Minerals Common on Asteroids."

Optics & Laser Technology, Vol. 135.

- [24] TransAstra. (2025). "Capture Bag." https://transastra.com/capabilities/capturing
- [25] Krasinsky, G.A., Pitjeva, E.V., Vasilyev, M.V., and Yagudina, E.I. (2002). "Hidden Mass in the Asteroid Belt." *Icarus*, Vol. 158, No. 1, pp. 98-105.
- [26] Steigerwald, W. (2013). "New NASA Mission to Help Us Learn How to Mine Asteroids." NASA. <a href="https://www.nasa.gov/solar-system/new-nasa-mission-to-help-us-learn-how-to-mine-asteroids/#:~:text=%E2%80%9CA%20small%2C%2010%2Dmeter%20(yard)%20S%2Dtype%20asteroid%20contains,metallic%20or%20%E2%80%9CM%2Dclass%E2%80%9D%20asteroids%2C%20according%20to%20Lauretta
- [27] MilliporeSigma. (2025). https://www.sigmaaldrich.com
- [28] Daily Metal Prices. (2025). https://www.dailymetalprice.com/
- [29] Ross, S.D. (2001). "Near-Earth Asteroid Mining" [Unpublished manuscript]. https://ross.aoe.vt.edu/papers/ross-asteroid-mining-2001.pdf
- [30] Relativity. (2025). "Terran R." https://www.relativityspace.com/terran-r
- [31] SpaceX. (2025). "Falcon 9." https://www.spacex.com/vehicles/falcon-9/
- [32] SpaceX. (2025). "Falcon Heavy." https://www.spacex.com/vehicles/falcon-heavy/
- [33] ULA. (2025). "Delta IV." https://www.ulalaunch.com/rockets/delta-iv
- [34] The European Space Agency. (2025). "Ariane 6 Overview." https://www.esa.int/Enabling Support/Space Transportation/Launch vehicles/Ariane 6 overview
- [35] NASA. (2025). "Space Launch System Core Stage." https://www.nasa.gov/wp-content/uploads/2020/09/sls core stage fact sheet 01072016.pdf
- [36] Stough, R.W., et al. (2021). "NASA's Space Launch System: Capabilities for Ultra-High C3 Missions." NASA. https://ntrs.nasa.gov/api/citations/20205007219/downloads/SLS-HelioDecadal-Paper-3page%20-%20BP%20FINAL.pdf
- [37] Blue Origin. (2025). "New Glenn: The Foundation for a New Era." https://www.blueorigin.com/new-glenn
- [38] World at Large. (2020). "TransAstra Enters Phase III for Prototyping Revolutionary Asteroid Mining Technologies." https://www.worldatlarge.news/2020/11/20/trans-astra-asteroid-mining-spacecraft-passes-1-year-nasa-review/
- [39] eoPortal (2013). "ISS: Cygnus." https://www.eoportal.org/satellite-missions/iss-cygnus
- [40] NASA. (2014). "An Alternate Orion Heat Shield Carrier Structural Design." https://www.nasa.gov/wpcontent/uploads/2015/05/orionheatshield.pdf
- [41] Russian Space Web. (2022). "RD-0146 Hydrogen Engine." https://www.russianspaceweb.com/rd0146.html
- [42] Monex Deposit Company. (2025). "Live Platinum Spot Prices." https://www.monex.com/platinum-prices/
- [43] Stickings, A. (2018). "SpaceX Falcon Heavy: That's No Moon ... It's A Tesla!" Rusi. https://www.rusi.org/explore-our-research/publications/rusi-defence-systems/spacex-falcon-heavy-thats-no-moon-its-tesla#:~:text=Perhaps%20the%20greatest%20benefit%20to,cheaper%20option%20for%20existing%20ones.
- [44] Sheetz. M. (2025). Blue Origin's First New Glenn Rocket Reaches Orbit, Misses Booster Landing." CNBC. https://www.cnbc.com/2025/01/16/jeff-bezos-blue-origin-new-glenn-rocket-launch.html

[45] Leonland. (2018) "Chemical Elements by Market Price." http://www.leonland.de/elements by price/en/list

[46] Statista. (2024) "Iron oxide price in the United States from 2013 to 2023." https://www.statista.com/statistics/881746/average-us-iron-oxide-price/

[47] U.S. Energy Information Administration. (2024) "Coal explained: Coal prices and outlook." https://www.eia.gov/energyexplained/coal/prices-and-outlook.php